

Search for neutron decoupling in ^{22}O via the $(d, d'\gamma)$ reaction

Z. Elekes,^{1,2} Zs. Dombrádi,¹ N. Aoi,² S. Bishop,² Zs. Fülöp,¹ J. Gibelin,³ T. Gomi,² Y. Hashimoto,⁴ N. Imai,² N. Iwasa,⁵ H. Iwasaki,⁶ G. Kalinka,¹ Y. Kondo,⁴ A. A. Korshennikov,^{2,7} K. Kurita,⁸ M. Kurokawa,² N. Matsui,⁴ T. Motobayashi,² T. Nakamura,⁴ T. Nakao,⁶ E. Yu. Nikolskii,^{2,7} T. K. Ohnishi,² T. Okumura,⁴ S. Ota,⁹ A. Perera,² A. Saito,⁶ H. Sakurai,² Y. Satou,⁴ D. Sohler,¹ T. Sumikama,² D. Suzuki,⁸ M. Suzuki,⁸ H. Takeda,⁶ S. Takeuchi,² Y. Togano,⁸ and Y. Yanagisawa²

¹*Institute of Nuclear Research of the Hungarian Academy of Sciences, P.O. Box 51, Debrecen, H-4001, Hungary*

²*Institute of Physical and Chemical Research, 2-1 Hirosawa, Wako, Saitama 351-0198, Japan*

³*Institut de Physique Nucléaire, 15 rue Georges Clemenceau, F-91406 Orsay, France*

⁴*Tokyo Institute of Technology, 2-12-1 Ookayama, Meguro-ku, Tokyo 152-8550, Japan*

⁵*Tohoku University, Sendai, Miyagi 9808578, Japan*

⁶*University of Tokyo, Tokyo 1130033, Japan*

⁷*Kurchatov Institute, Kurchatov sq. 1, RU-123182, Moscow, Russia*

⁸*Rikkyo University, 3 Nishi-Ikebukuro, Toshima, Tokyo 171, Japan*

⁹*Kyoto University, Kyoto 606-8501, Japan*

(Received 9 May 2006; published 19 July 2006)

We have searched for valence neutron decoupling in ^{22}O , a phenomenon recently observed in neutron-rich C, B, and lighter O nuclei. From the cross section of the $(d, d'\gamma)$ reaction for the transition between the ground state and the first 2^+ state of ^{22}O , the neutron and proton deformation parameters have been deduced by distorted wave analysis using and reanalyzing the data of a previous Coulomb excitation measurement. The ratio of the neutron and proton multipole transition matrix elements M_n/M_p compared to the N/Z value has been derived to be around 1. This result indicates that the ^{22}O isotope has small and similar neutron and proton deformations, which is consistent with $N = 14$ shell closure. Thus, the concept of neutron decoupling does not hold for this nucleus.

DOI: [10.1103/PhysRevC.74.017306](https://doi.org/10.1103/PhysRevC.74.017306)

PACS number(s): 23.20.Js, 25.45.De, 25.60.-t, 27.30.+t

During the last few years a deep interest has evolved to explore the unusual features of very neutron-rich nuclei. A possible dripline effect is the development of a thick neutron skin [1], the concept of which is needed also to interpret the Coulomb displacement energies in mirror nuclei [2]. Increasing the number of neutrons in a nucleus causes the nuclear radius to grow according to the $A^{1/3}$ rule, while the size of the proton distribution may remain nearly constant. Such a situation was found, e.g., in heavy Na isotopes, where a neutron skin of ~ 0.4 fm was observed [3]. The consequence of a neutron skin may be special dripline features. According to theoretical calculations, the most specific excitation mode of nuclei with a thick neutron skin is the isoscalar quadrupole excitation of the skin, which is a large-amplitude motion decoupled from the rest of the nucleus [4,5]. Recently, as a result of incorporation of the continuum coupling into the quasiparticle random phase approximation, calculations predicted a surface neutron quadrupole mode associated with a bound 2^+ state [6–8]. The strength of the neutron contribution is expected to be proportional to the number of neutrons in the neutron skin [6,7]. In self-consistent calculations, where the effect of the shell closure is also taken into account [8], a bell-shaped strength distribution as a function of mass is predicted similar to the mass dependence of the quadrupole electromagnetic transition probability, but the neutron strength is calculated to be several times larger than the electromagnetic one for the oxygen isotopic chain.

Indeed, a significant enhancement of the neutron transition probability has been measured both for ^{18}O and ^{20}O [9,10].

Both from experimental systematics [9] and theoretical considerations [8], a large neutron transition probability is expected also for ^{22}O . To observe the evolution of nuclear structure effects as the dripline is approached at ^{24}O , we studied the neutron transition probability in ^{22}O by use of the $(d, d'\gamma)$ process. In a parallel work, the (p, p') reaction [which has a different sensitivity for protons and neutrons than the (d, d') probe] was applied [11] for this purpose.

In our experiment, a 94A MeV energy primary beam of ^{40}Ar with 60 pA intensity hit a ^9Be production target of 0.3 cm thickness. The reaction products were momentum and mass analyzed by the Institute of Physical and Chemical Research (RIKEN) projectile fragment separator (RIPS) [12]. The RIPS was operated at 6% momentum acceptance. The secondary beam mainly included neutron-rich ^{25}Ne and ^{22}O nuclei. The total intensity was approximately 1500 cps having an average ^{22}O intensity of 600 cps. The identification of incident beam species was performed by energy loss and time of flight (TOF). Two plastic scintillators of 1 mm thickness were placed at the first and second focal planes (F2 and F3) to measure the TOF. Silicon detectors with thickness of 0.5 mm were inserted at F2 and F3 for energy loss determination. The separation of ^{22}O particles was complete. The secondary beam was transmitted to a CD_2 target of 30 mg/cm² at the final focus of RIPS. The reaction occurred at an energy of 34A MeV. The position of the incident particles was determined by two parallel plate avalanche counters (PPACs) placed at F3 upstream of the target. The scattered particles were detected and identified by a 2×2 matrix silicon telescope placed 96 cm

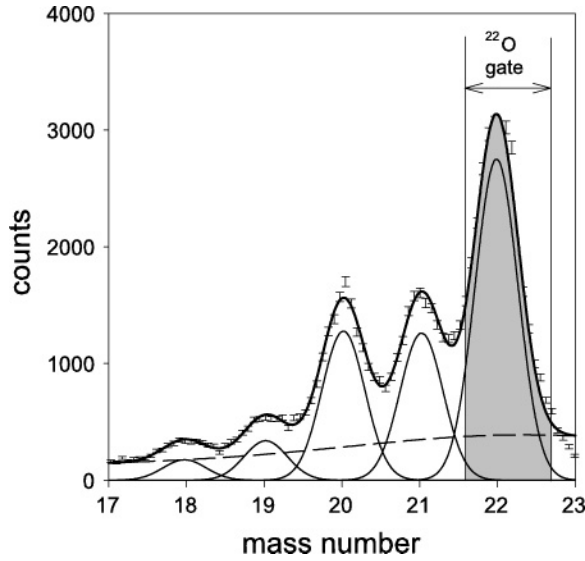


FIG. 1. Separation of oxygen isotopes using ΔE - E information in the silicon telescope. Bold solid line is a sum of five Gaussian functions and a polynomial background. The individual Gaussians and the background function are also plotted with the thin and dashed solid lines, respectively.

downstream of the target. The telescope consisted of four layers with thicknesses of 0.5, 0.5, 2, and 2 mm. The first two layers were made of stripped detectors measuring the x and y positions of the fragments. On the basis of ΔE - E information, separation was carried out among the different oxygen isotopes, which is demonstrated in Fig. 1, where the linearized mass spectrum of oxygen nuclei is shown for one segment of the telescope.

Eighty NaI(Tl) scintillator detectors of the Detector Array for Low Intensity radiation (DALI) array [13] surrounded

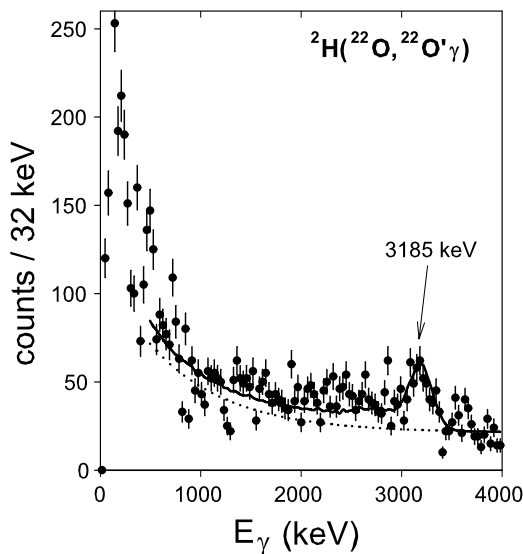


FIG. 2. Doppler-corrected spectra of γ rays emerging from $^{22}\text{O}+\text{CD}_2$ reaction. Solid line is the final fit including the spectrum curve from GEANT4 simulation; an additional smooth polynomial background is plotted as a dotted line.

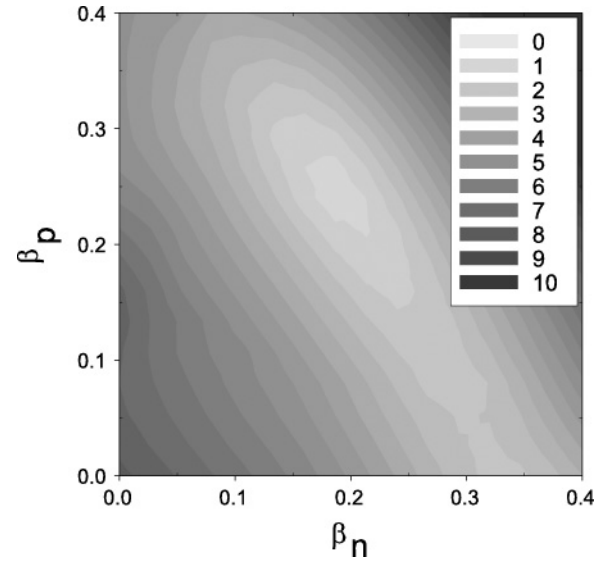


FIG. 3. Two-dimensional plot of β_p vs β_n with parameter set (1). The contours are χ^2 values representing the difference between the calculated and experimental cross sections for the $(^{197}\text{Au}, ^{197}\text{Au})$ and (d, d') process.

the target to detect the deexciting γ rays emitted by the inelastically scattered nuclei. The intrinsic energy resolution of the array was 10% (full width at half maximum) for a 662 keV γ -ray energy. Figure 2 present the Doppler-corrected γ ray spectra for ^{22}O nucleus, which were produced by putting a gate on the time spectra of the NaI(Tl) detectors selecting the prompt events and subtracting the random coincidences. By first fitting the spectrum with a Gaussian function and smooth exponential background, the position of the single peak was determined at 3185(15) keV. The quoted uncertainty of the peak position is the square root of the sum of the squared uncertainties including two main errors, namely, the statistical one and the one due to Doppler correction. The above energy for ^{22}O is in a good agreement with the value 3199(8) keV measured earlier [14].

After the peak position was determined, it was fed into the detector simulation software GEANT4 [17], and the resultant response curve plus a smooth polynomial background was used to analyze the experimental spectrum and determine the angle-integrated cross section for the $^{22}\text{O}+^2\text{H}$ reaction to be $\sigma(0_1^+ \rightarrow 2_1^+) = 19 \pm 3$ mb. We note that the contribution from the $^{22}\text{O}+^{12}\text{C}$ reaction was obtained by analyzing the mass spectrum of the recoiled particles, i.e., the target nuclei, and found to be 10%. This result can be combined

TABLE I. Neutron and proton deformations of ^{22}O and M_n/M_p values normalized with N/Z ratio derived by using different optical potential parameter sets.

Optical potential parameter set	β_n	β_p	$(M_n/M_p)/(N/Z)$
1 [15]	0.20 ± 0.06	0.24 ± 0.07	0.9 ± 0.3
2 [16]	0.29 ± 0.07	0.22 ± 0.07	1.3 ± 0.5

with the data from the $^{22}\text{O}+^{197}\text{Au}$ reaction [18], where the sensitivity of the probe for proton and neutron distributions is different from that of our case. First, we took different pairs of neutron and proton deformation parameters ($\beta_n = \delta_n/R$, $\beta_p = \delta_p/R$; R is the nuclear radius) and converted them to matter and Coulomb deformation lengths for the deuteron and gold probes (δ_M^d , δ_M^{Au} , and $\delta_C = \delta_p$) using the formulas

$$(Nb_n^d + Zb_p^d)\delta_M^d = Nb_n^d\delta_n + Zb_p^d\delta_p, \quad (1)$$

$$(Nb_n^{\text{Au}} + Zb_p^{\text{Au}})\delta_M^{\text{Au}} = Nb_n^{\text{Au}}\delta_n + Zb_p^{\text{Au}}\delta_p, \quad (2)$$

where N and Z are the neutron and proton numbers, respectively, while $b_n^d/b_p^d = 1$ and $b_n^{\text{Au}}/b_p^{\text{Au}} = 0.82$ are the sensitivity parameters for neutrons and protons of the (d , d') and (^{197}Au , $^{197}\text{Au}'$) probes. In the next step, the matter and Coulomb deformation parameters were put into a distorted wave calculation performed by ECIS97 [19]. The resulting calculated cross sections were compared to the experimental ones, and χ^2 values were determined for each pair of neutron and proton deformation parameters. During the (re)analysis, the same optical potential parameters of Ref. [18] were used for the scattering on ^{197}Au , while two sets of parameters ([1] $^{16}\text{O}+^2\text{H}$ at 31.6A MeV in [15], and [2] $^{22}\text{Ne}+^2\text{H}$ at 26.0A MeV in [16]) were employed for the (d , d') reaction. A two-dimensional plot of β_p vs β_n with parameter set (1) is shown in Fig. 3, where the contours are χ^2 values representing the difference between the calculated and experimental cross sections. The role of the neutron and proton excitations in the 2_1^+ state can be characterized further by the neutron and proton multipole transition matrix elements M_n and M_p , which are determined as [20]

$$\frac{M_n}{M_p} = \frac{b_p}{b_n} \left(\frac{\delta_M}{\delta_C} \left(1 + \frac{b_n N}{b_p Z} \right) - 1 \right). \quad (3)$$

The derived deformation parameters together with the

(M_n/M_p)/(N/Z) ratios can be found in Table I. It can be clearly seen that the dependence on the choice of the optical parameters is small, and the neutron and proton deformations are close to each other. The (M_n/M_p)/(N/Z) ratio is 0.9 ± 0.3 and 1.3 ± 0.5 for the two parameter sets, which are consistent with each other and with a recent result of 1.4 ± 0.5 obtained by a microscopic analysis based on matter and transition densities generated by continuum Skyrme-Hartree-Fock-Bogoliubov and quasiparticle random phase approximation calculations, respectively [11].

The deformations deduced are similar to that of ^{16}O , reflecting that both the proton and neutron shells are also closed in ^{22}O . This is in contrast with the situation of ^{20}O , where the increased neutron matrix elements were ascribed to larger neutron deformation or stiffness. While mean field calculations account for the $N = 16$ subshell closure and predict a significant decrease in the quadrupole transition strengths [8], they cannot describe the $N = 14$ subshell closure, which blocks the surface oscillations of the valence neutrons in ^{22}O .

Summarizing our results, we have studied the ^{22}O nucleus in the (d , $d'\gamma$) reaction. From the excitation cross section of the 2_1^+ state, using and reanalyzing the results of a previous (^{197}Au , $^{197}\text{Au}'$) measurement, the ratio of the neutron and proton multipole transition matrix elements (M_n/M_p)/(N/Z) was determined to be around 1, this confirmed a recent result for the $N = 14$ shell closure by Becheva *et al.* [11]. Unlike the case of ^{20}O , the 2_1^+ state of ^{22}O cannot be assigned to surface vibration of the neutron skin.

We thank Dr. Y. Maeda for his help in preparing the CD_2 target. The present work was partly supported by the Grant-in-Aid for Scientific Research (No. 1520417) by the Japan Ministry of Education, Culture, Sports, Science, and Technology and by OTKA T42733, T46901, and F60348.

-
- [1] I. Tanihata, D. Hirata, T. Kobayashi, S. Shimoura, K. Sugimoto, and H. Toki, Phys. Lett. **B289**, 261 (1992).
[2] J. Duflo and A. P. Zuker, Phys. Rev. C **66**, 051304 (2002).
[3] T. Suzuki, H. Geissel, O. Bochkarev, L. Chulkov, M. Golovkov, D. Hirata, H. Irnich, Z. Janas, H. Keller, T. Kobayashi *et al.*, Phys. Rev. Lett. **75**, 3241 (1995).
[4] M. Yokoyama, T. Otsuka, and N. Fukunishi, Phys. Rev. C **52**, 1122 (1995).
[5] H. Sagawa, Phys. Rev. C **65**, 064314 (2002).
[6] M. Matsuo, Nucl. Phys. **A696**, 371 (2001).
[7] M. Matsuo, Prog. Theor. Phys. Supp. **146**, 110 (2002).
[8] E. Khan, N. Sandulescu, M. Grasso, and N. V. Giai, Phys. Rev. C **66**, 024309 (2002).
[9] J. Jewell, L. Riley, P. Cottle, K. Kemper, T. Glasmacher, R. Ibbotson, H. Scheit, M. Chromik, Y. Blumenfeld, S. Hirzebruch *et al.*, Phys. Lett. **B454**, 181 (1999).
[10] E. Khan, Y. Blumenfeld, V. Nguyen, T. Suomijarvi, N. Alamanos, F. Auger, G. Colo, N. Frascaria, A. Gillibert, T. Glasmacher *et al.*, Phys. Lett. **B490**, 45 (2000).
[11] E. Becheva, Y. Blumenfeld, E. Khan, D. Beaumel, J. Daugas, F. Delaunay, C.-E. Demonchy, A. Drouart, M. Fallot, A. Gillibert *et al.*, Phys. Rev. Lett. **96**, 012501 (2006).
[12] T. Kubo, M. Ishihara, N. Inabe, H. Kumagai, I. Tanihata, K. Yoshida, T. Nakamura, H. Okuno, S. Shimoura, and K. Asahi, Nucl. Instrum. Methods B **70**, 309 (1992).
[13] S. Takeuchi, T. Motobayashi, H. Murakami, K. Demichi, and H. Hasegawa, RIKEN Accel. Prog. Rep. **36**, 148 (2003).
[14] M. Stanoiu, F. Azaiez, Z. Dombradi, O. Sorlin, B. Brown, M. Belleguic, D. Sohler, M. S. Laurent, M. Lopez-Jimenez, Y. Penionzhkevich *et al.*, Phys. Rev. C **69**, 034312 (2004).
[15] M. Cooper, W. Hornyak, and P. Roos, Nucl. Phys. **A218**, 249 (1974).
[16] F. Hinterberger, G. Mairle, U. Schmidt-Rohr, G. Wagner, and P. Turek, Nucl. Phys. **A115**, 570 (1968).
[17] S. Agostinelli, J. Allison, K. Amako, J. Apostolakis, H. Araujo, P. Arce, M. Asai, D. Axen, S. Banerjee, G. Barrand, *et al.*, Nucl. Instrum. Methods A **506**, 250 (2003).
[18] P. Thirof, B. Pritychenko, B. Brown, P. Cottle, M. Chromik, T. Glasmacher, G. Hackman, R. Ibbotson, K. Kemper, T. Otsuka, *et al.*, Phys. Lett. **B485**, 16 (2000).
[19] J. Raynal, Phys. Rev. C **23**, 2571 (1981).
[20] A. M. Bernstein, V. R. Brown, and V. A. Madsen, Phys. Rev. Lett. **42**, 425 (1979).